PNAS
www.pnas.org

Supplementary Information for

HIM-17 regulates the position of recombination events and GSP-1/2 localization to establish short arm identity on bivalents in meiosis

Saravanapriah Nadarajan[1], Elisabeth Altendorfer[1], Takamune T. Saito[1,2], Marina Martinez-Garcia[1], and Monica P. Colaiácovo[1]*

[1]Department of Genetics, Harvard Medical School, Boston, MA 02115, USA.

[2]Current Address: Department of Genetic Engineering, Faculty of Biology-Oriented Science and Technology, Kindai University, Wakayama 649-6493, Japan.

***Correspondence:** mcolaiacovo@genetics.med.harvard.edu; Phone: 617-432-6543; Fax: 617-432-7663.

This PDF file includes:

Supplementary text
Figures S1 to S3
Tables S1 to S2
SI References

Supplementary Information Text

Materials and Methods

Antibodies

C. elegans gonads were dissected in EGG buffer and fixed with 1% paraformaldehyde for 5 min, freeze cracked and treated with ice cold methanol for 1 min. All primary antibodies were used at the following dilutions for immunofluorescence: chicken α-GFP (1:400; Abcam), rabbit α-SYP-1 (1:200; 1), guinea pig α-HTP-3 (1:400; 2), rabbit α-RAD-51 (1:10,000; Novus Biological (SDI), rabbit α-AIR-2 (1:100; 3, 4), rabbit α-LAB-1 (1:300; 4), mouse α-H3K9me2 (1:500; Abcam) and rabbit anti-H3 pT3 (1:700; Merck Millipore; 5). The following secondary antibodies from Jackson ImmunoResearch were used at a 1:200 dilution: α-chicken Alexa 488, α-rabbit Cy3, α-mouse Alexa 488, and α-guinea pig Alexa 488. Vectashield containing 1μg/μl of DAPI from Vector Laboratories was used as a mounting media and anti-fading agent.

Immunofluorescence and imaging

Whole mount preparation of dissected gonads and immunostaining procedures were performed as in (6). Immunofluorescence images were captured with an IX-70 microscope (Olympus) fitted with a cooled CCD camera (CH350; Roper Scientific) driven by the Delta Vision system (Applied Precision). 10X ocular lenses and 60X and 100X objective lenses were used for imaging. Optical sections were collected at 0.20 μm increments and deconvolved using the SoftWorx 3.0 deconvolution software from Applied Precision. All quantification data for immunostainings and complete statistical analysis is shown in Dataset S1.

RNA interference

RNAi was performed as in (7) with the following modifications: three L4-stage animals were placed on each RNAi plate and next generation, 24 hours post-L4 animals were screened for phenotype. HT115 bacteria expressing empty pL4440 vector was used as the control RNAi.

Irradiation experiments

For the analysis of bivalents at diakinesis, young (~18 hours post-L4 stage) wild type and *him-17* mutant adult animals were irradiated with approximately 60 Gy from a Cs^{137} source. Irradiated and untreated control worms were dissected 24 hours post-irradiation for immunostaining, allowing for sufficient time for nuclei undergoing DSBs earlier in prophase I to progress into diakinesis for analysis. For the analysis of computationally straightened chromosomes in pachytene, 22 to 24 hours post-L4 wild type and *him-17* mutant adult animals were irradiated with 60 Gy from a Cs^{137} source. Irradiated and untreated control worms were dissected 1 hour post-irradiation for immunostaining, when the maximum number of RAD-51 foci are detected post-IR.

RAD-51 Time Course Analysis

Quantitative analysis of RAD-51 foci/nucleus was performed as in (6). The number of nuclei scored per zone (n) for a given genotype is listed in Dataset S1. Statistical comparisons between genotypes were conducted using the two-tailed Mann-Whitney test, 95% C.I.

Generation of *gsp-1* phosphodead and phosphomimetic mutants by CRISPR/Cas9 genome editing

To generate the phosphodead *gsp-1(S2A)* mutant, the serine at position 2 was mutated to alanine. To generate the phosphomimetic *gsp-1(S2D)* mutant, the serine at position 2 was mutated to glutamic acid. We used the following guide RNA sequence: gcaaaaacaAUGUCGAACGAUGG. The following template oligo sequence was used to generate the phosphodead *gsp-1 (S2A)* mutant: atcaaaagtgaccaacagaagccgcggagattgcagctgcaaaaacaATGGCCAACGATGGAGATTTAAACATT GACAATCTGATCACCAGACTTCTTGAAGgtg. The following template oligo sequence was used to generate the phosphomimetic *gsp-1(S2D)* mutant: atcaaaagtgaccaacagaagccgcggagattgcagctgcaaaaacaATGGAAAACGATGGAGATTTAAACATT GACAATCTGATCACCAGACTTCTTGAAGgtg.

CO distribution mapping

Meiotic crossover frequencies and distribution were assayed utilizing single-nucleotide polymorphism (SNP) markers as in (8). The SNP markers located at the boundaries of the chromosome domains were chosen based on data from WormBase (WS231) and (9). The SNP markers and primers used for chromosomes III and X are indicated in Table S2 and (10), respectively. PCR and restriction digests of single egg lysates were performed as described in (11, 12). Statistical analysis was performed using the two-tailed Fisher's Exact test as in (13, 14). Quantification and statistical analysis is shown in Dataset S1.

Mass spectrometry analysis of immunoprecipitation experiments

Two independent immunoprecipitations were performed using 24h post-L4 synchronized HIM-17::GFP and wild-type worms. Animals were collected, frozen in liquid nitrogen and homogenized by sonication as in (15). Anti-GFP conjugated agarose beads (MBL, Catalog # D153-8) were used for immunoprecipitation. The proteoExtract protein precipitation kit (Calbiochem, #539180) was used followed by mass spectrometry analysis (Taplin Biological Mass Spectrometry Facility, HMS, MA) to identify HIM-17::GFP interacting proteins. Hits were first curated by internal normalization (number of total peptides of a protein over total number of peptides per sample). For proteins that appear in both HIM-17::GFP and control pulldowns, this was followed by calculation of fold-change enrichment with respect to their presence in the controls.

Effect size calculation

The relative risk and odds ratio was calculated to measure the effect size for data where a Fisher’s Exact test was applied to assess statistical significance. Effect sizes are shown in the Dataset S1.

A

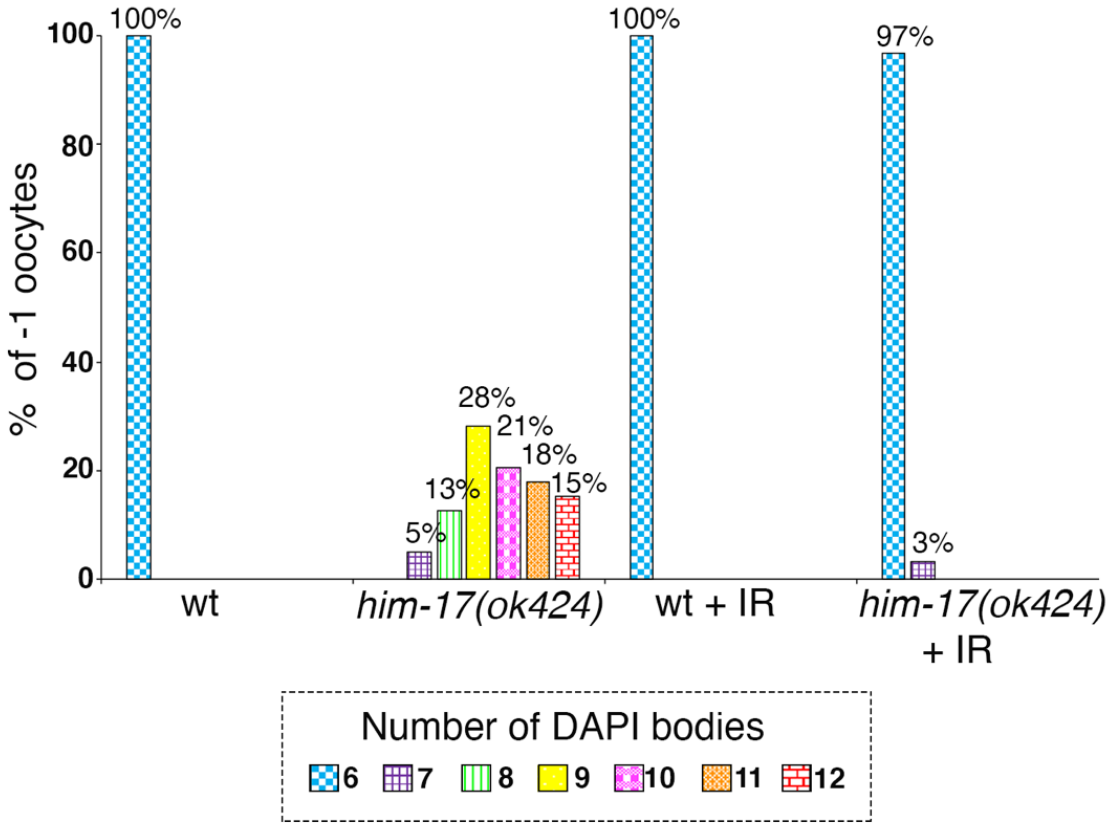
100%
100%
97%
28%
21%
18%
15%
13%
5%
3%
% of -1 oocytes
100
80
60
40
20
0
wt
him-17(ok424)
wt + IR
him-17(ok424) + IR
Number of DAPI bodies
6
7
8
9
10
11
12

B

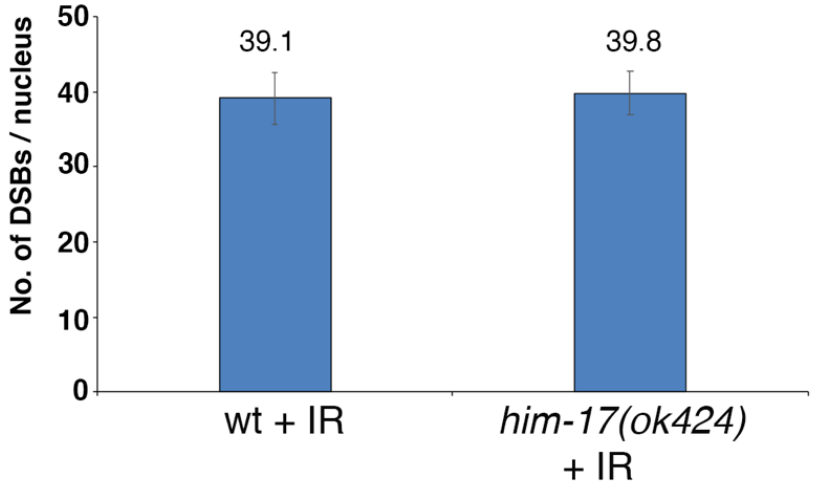
No. of DSBs / nucleus
50
40
30
20
10
0
39.1
39.8
wt + IR
him-17(ok424) + IR

Fig. S1. Distribution of DAPI bodies in wild type and *him-17* mutant. (A) Histogram showing the percentage distribution of number of DAPI bodies observed in -1 oocytes in wild type, wildtype + IR, *him-17(ok424)* null mutant, and *him-17(ok424)* null mutant + IR. 6 DAPI bodies corresponds to six bivalents, 12 DAPI bodies corresponds to 12 univalents, and 7 to 11 DAPI bodies correspond to combinations of between 5 to 1 bivalent, respectively, and univalents. -1 oocytes of 35, 78, 21 and 30 animals were analyzed for wild type, wildtype + IR, *him-17(ok424)*, and *him-17(ok424)* + IR, respectively. (B) Histogram showing the number of DSBs detected per pachytene nucleus by RAD-51 immunostaining after exposure to γ-IR (60 Gy) in wild type and *him-17* mutant. 97 nuclei from 4 animals were analyzed for each genotype.

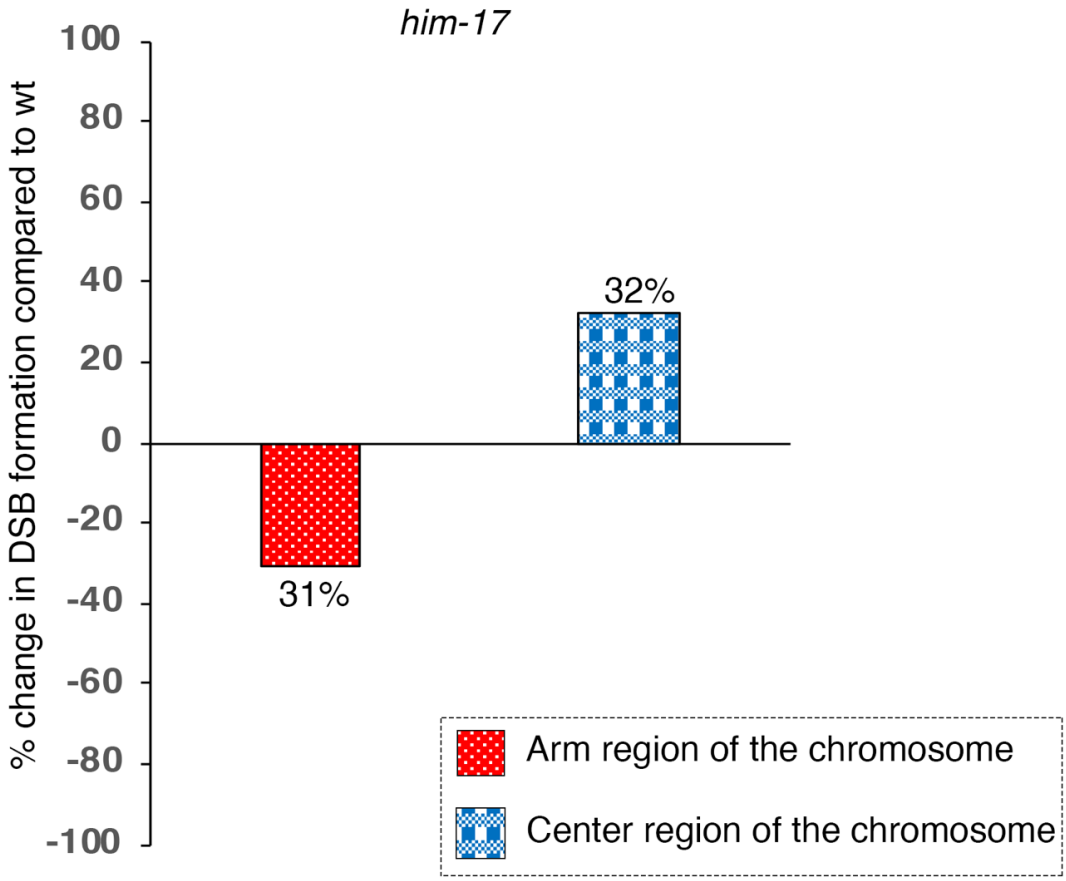
him-17
100
80
60
40
20
0
-20
-40
-60
-80
-100
% change in DSB formation compared to wt
32%
31%
Arm region of the chromosome
Center region of the chromosome

Fig. S2. Change in the pattern of DSB-dependent RAD-51 foci formation on the chromosomes in *him-17* mutant. Histogram showing the changes in the pattern of DSB-dependent RAD-51 foci formation on the arm versus center region of the chromosomes in the *him-17* mutant compared to wild type. There is a 31% decrease in the number of DSB-dependent RAD-51 foci on the arm region and a 32% increase on the center region of the chromosomes relative to the total number of DSB-dependent RAD-51 foci detected compared to wild type.

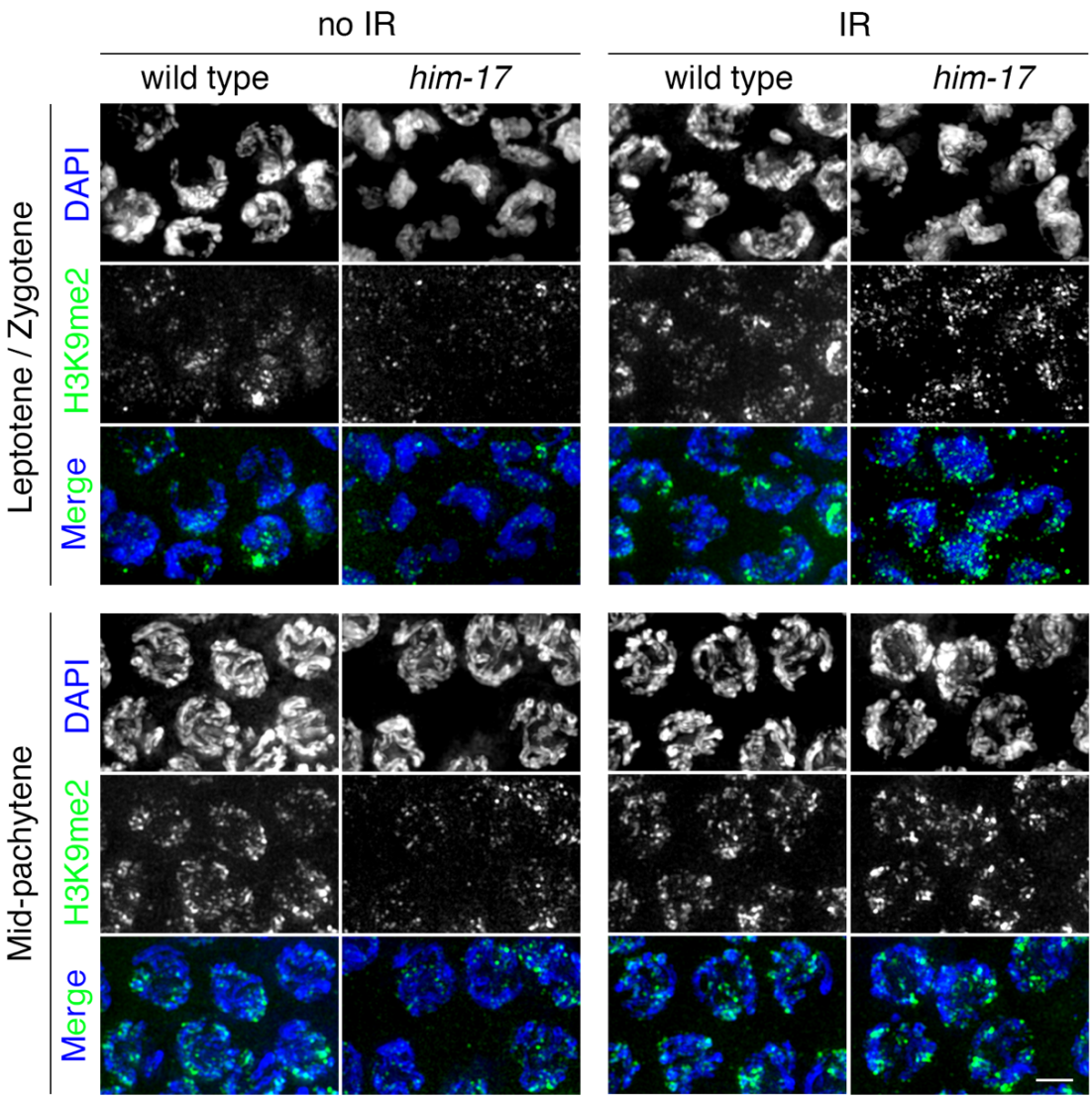
no IR
IR
wild type
him-17
wild type
him-17
Leptotene / Zygotene
DAPI
H3K9me2
Merge
Mid-pachytene
DAPI
H3K9me2
Merge

Fig. S3. Reduced H3K9me2 signal in the germlines of *him-17* mutants is rescued by γ-IR. High-magnification images of leptotene/zygotene (top) and mid- pachytene stage (bottom) nuclei in wild type and *him-17* gonad arms treated or not with γ-IR (60 Gy). Co-staining with anti-H3K9me2 (green) and DAPI (blue) shows that H3K9me2 signal is reduced in *him-17* mutants compared to wild type and this signal can be rescued by exposure to γ-IR. Two gonad arms were analyzed for each genotype. Scale bar, 2 μm.

Table S1. Immunoprecipitation (IP) from HIM-17::GFP whole worm extracts with an antibody against GFP analyzed by mass spectrometry.

Protein ID	Protein name/ORF	Fold-change	Sequence Coverage (%)
CE13489	HIM-17	Specific	42.20
	GFP	Specific	60.50
CE30816	MEK-1	Specific	9.30
CE01405	KIN-18	Specific	2.30
CE24993	F52B5.2	Specific	7.60
CE38356	KIN-20	Specific	4.80
CE26649	PLK-1	5.39	8.60
CE21025	AIR-1	3.29	22.70
CE20735	GSP-1	2.39	11.60
CE00315	CDK-1	2.20	44

Fold-change indicates the specificity or the level of enrichment of peptides for each protein found in HIM-17::GFP IP samples, with respect to the control samples. A cut-off of 2-fold or higher was used to select for interactors. The selection of candidate kinases was based on their robust and specific expression in the germline or in previously described roles during meiosis. Sequence coverage refers to the percentage of the protein sequence that was pulled down in the HIM-17::GFP IP samples.

Table S2. SNP markers and primers used in the snip-SNP analysis comparing crossover distribution between wild type and *him-17* mutants

Chr.	Position (kb)	SNP	Primers	Enzyme	Bristol digest (bp)	Hawaiian digest (bp)
III	A (158)	pKP3081	AGCAAGAATGAGCCGATTG GTCGGCCGTTTTCAAATAACTG	*Taq*I	222, 150	195, 150, 27
	B (3,749)	F34D10 at position 20673	CCATCGATTTTGTCCTGG AACAATGGCTCCGTGATG	*Mse*I	325, 67, 44, 42,9	240,85,67, 44, 42, 9
	C (10,653)	snp_Y39A l	AGCGTTAAAGTATCGGTTATTTCG TAAATTCATTTCAAACAATCGAGC	*Dra*I	355, 142, 30	497, 30
	D (13,715)	uCE3-1426	AGCAGGCTCACCATCATCATCA GACATTACGGTAGAGGAGATGGA	*Dra*I	273, 137, 78	200, 137, 78, 73
X	A (535)	pKP6100	TGGCAAAACACATCCCTGTG GGTATCCGATCCCTTCAACAAG	*Bsp*HI	208, 156	364
	B (6,152)	pKP6108	AGCAATCTGGATATGCAAATCC GAATACTCGGAGCGGTGCCA	*Nsi*I	488, 85	573
	C (12,208)	pKP6125	ACAGTAAGATGACCATACACACG AAGCAGCGCGAGGTATGTAG	*Taq*I	308	210, 98
	D (17,701)	pKP6172	TTCTGTTGATTTGGTTGCTCCG TGATGCAGGAACAAAAGTAGTG	*Apo*I	174, 117	291

SI References

1. MacQueen AJ, Colaiácovo MP, McDonald K, Villeneuve AM (2002) Synapsis-dependent and -independent mechanisms stabilize homolog pairing during meiotic prophase in *C. elegans*. *Genes Dev* 16(18):2428–2442.

2. Goodyer W, et al. (2008) HTP-3 links DSB formation with homolog pairing and crossing over during *C. elegans* meiosis. *Dev Cell* 14(2):263–274.

3. de Carvalho CE, Colaiácovo MP (2006) SUMO-mediated regulation of synaptonemal complex formation during meiosis. *Genes Dev* 20(15):1986–1992.

4. de Carvalho CE, et al. (2008) LAB-1 antagonizes the Aurora B kinase in *C. elegans*. *Genes Dev* 22(20):2869–2885.

5. Ferrandiz N, et al. (2018) Spatiotemporal regulation of Aurora B recruitment ensures release of cohesion during *C. elegans* oocyte meiosis. *Nat Commun* 9(1):834.

6. Colaiácovo MP, et al. (2003) Synaptonemal complex assembly in *C. elegans* is dispensable for loading strand-exchange proteins but critical for proper completion of recombination. *Dev Cell* 5(3):463–474.

7. Govindan JA, Cheng H, Harris JE, Greenstein D (2006) Gα o/i and Gα s signaling function in parallel with the MSP/Eph receptor to control meiotic diapause in *C. elegans*. *Curr Biol* 16(13): 1257-68.

8. Nabeshima K, Villeneuve AM, Hillers KJ (2004) Chromosome-wide regulation of meiotic crossover formation in *Caenorhabditis elegans* requires properly assembled chromosome axes. *Genetics* 168(3):1275–1292.

9. Rockman MV, Kruglyak L (2009) Recombinational landscape and population genomics of *Caenorhabditis elegans*. *PLoS Genet* 5(3):e1000419.

10. Saito TT, Lui DY, Kim H-M, Meyer K, Colaiácovo MP (2013) Interplay between structure-specific endonucleases for crossover control during *Caenorhabditis elegans* meiosis. *PLoS Genet* 9(7):e1003586.

11. Davis MW, et al. (2005) Rapid single nucleotide polymorphism mapping in *C. elegans*. *BMC Genomics* 6(1):118.

12. Smolikov S, Schild-Prufert K, Colaiácovo MP (2008) CRA-1 uncovers a double-strand break-dependent pathway promoting the assembly of central region proteins on chromosome axes during *C. elegans* meiosis. *PLoS Genet* 4(6):e1000088.

13. Mets DG, Meyer BJ (2009) Condensins regulate meiotic DNA break distribution, thus crossover frequency, by controlling chromosome structure. *Cell* 139(1):73–86.

14. Meneely PM, McGovern OL, Heinis FI, Yanowitz JL (2012) Crossover distribution and frequency are regulated by him-5 in *Caenorhabditis elegans. Genetics* 190(4):1251–1266.

15. Nadarajan S, Govindan JA, McGovern M, Hubbard EJA, Greenstein D (2009) MSP and GLP-1/Notch signaling coordinately regulate actomyosin-dependent cytoplasmic streaming and oocyte growth in *C. elegans*. *Development* 136(13):2223–2234.